Computer simulations of quasilattice models for novel ferroelectric liquid crystals

Dennis R. Perchak*
Computational Science Laboratory, Research Laboratories, Eastman Kodak Company, Rochester, New York 14650-2216

Rolfe G. Petschek
Department of Physics, Case Western Reserve University, Cleveland, Ohio 44106-2623
(Received 2 January 1991)

It has been suggested that ferroelectric smectic phases may be formed by "fraternal-twin" liquid-crystal molecules, consisting of two very different mesogens bonded together by an appropriate spacer [R. G. Petschek and K. M. Wiefling, Phys. Rev. Lett. **59**, 343 (1987)]. We discuss the range in which these ferroelectric phases appear in a Monte Carlo simulation of a simple computer model for such mesogens. The mesogens consist of two identical flexible segments that are bonded to two rigid segments with very different lengths which, in turn, are bonded together by a flexible segment. In the computer model these monomers can move freely in one direction, but are constrained to lie on a hexagonal lattice of rods in the other two directions, roughly the packing expected in a smectic-*B* crystal. The flexible segments are modeled by springs, and there is an energy cost for the overlap of flexible and rigid segments on neighboring lattice rods. The region in which polar (flexible, short rigid, flexible, long rigid, flexible) smectic layers form will be discussed.

I. INTRODUCTION

A variety of small molecules (mesogens),[1,2] block copolymers,[3,4] and polymers made up of mesogens[5,6] form liquid-crystalline phases. Many mesogens have symmetries consistent with the formation of ferroelectric phases and nonzero dipole moments so there is no fundamental reason that ferroelectric phases should not exist. However, only the chiral smectic-*C* phase and related tilted smectic phases have been observed to be ferroelectric.[7] Even this phase can be rigorously considered to be ferroelectric only in two dimensions because the direction of the polarization varies helically through the sample in three dimensions. Ferroelectric phases are typically not the lowest free-energy phases of known mesogens, presumably because the intermolecular forces are too weak to align the mesogens parallel to each other or tend to align the mesogens antiparallel to one another. Recently, several authors[8–10] have suggested molecular architectures that may be capable of forming ferroelectric liquid-crystalline phases and yet would be nonchiral. Petschek and Wiefling[8] (hereafter to be referred to as I) have proposed that ferroelectric smectic phases may be formed by "fraternal-twin" liquid-crystal molecules, consisting of two very different mesogens bonded together by an appropriate spacer. Palffy-Muhoray, Lee, and Petschek[9] have examined the possible ferroelectric phases of disk-shaped molecules with appropriate electric dipole interactions. Finally, Lin Lei[10] has suggested the use of "bowl-shaped" molecules as the means to align mesogens. It is the purpose of the present investigation to begin computer-simulation studies of some of these ideas. In particular, we examine the suggested molecular architectures of paper I.

The basic idea in I is to form a layered phase with three or more sublayers, *A*,*B*,*C* so that the layers occur in an ordered fashion throughout the system, i.e., *ABCABCABC* (Fig. 1). If the *B* layer contained a dipole pointing towards the *A* layer, then the system would be ferroelectric. The different parts of the molecule must be

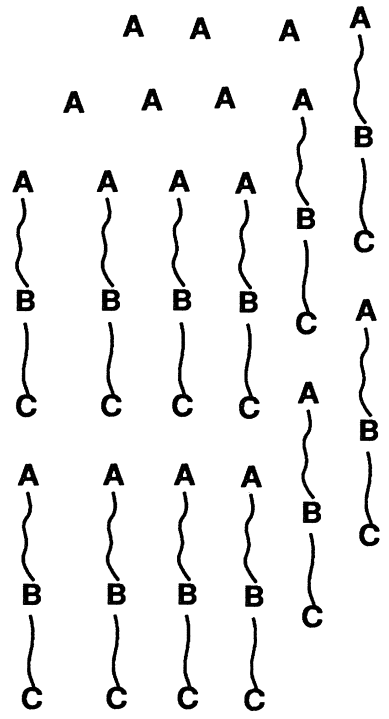

FIG. 1. Schematic of the layered, ferroelectric structure as proposed in paper I. The symbols *A*, *B*, and *C* stand for different moieties, e.g., three very different liquid-crystal-forming molecules. They are bonded together with flexible spacers. If there is a dipole pointing from the *B* monomer to the *A* monomer, then the phase will be ferroelectric.

sufficiently incompatible chemically and/or sterically to bring about this layering. Moreover, since the structure has the dipoles within a layer side by side and parallel, the layering incompatibility (i.e., the interactions which drive the formation of the sublayers) must be sufficiently large to overcome the unfavorable parallel arrangement of the dipoles. It can also be shown that interlayer Coulombic interactions will favor the ferroelectric *ABCABC* ordering rather than the antiferroelectric *ABCCBA* one.[8] Paper I discusses several possible molecular architectures that would result in a ferroelectric phase. One is to use combinations of rigid-rod moieties (e.g., biphenyls) with flexible moieties (e.g., alkane chains). Such mesogens are expected to form layered phases with two types of layers or other microstructures. By using various lengths for each segment, the molecule can be made so that not all segments of the same type are compatible.

The computer simulation of liquid-crystal-forming fluids is a rapidly growing field and already has a rich history.[11–25] Simulations range from (relatively) simple lattice models of liquid crystals and amphiphilic systems to complex all-atom-type potentials. An early model was that of Lebwohl and Lasher.[12–14] The model consisted of uniaxial particles confined to a cubic lattice with a potential interaction dependent upon the second Legendre polynomial of the cosine of the relative angle between the axes of nearest-neighbor particles. Such an interaction is simple and consistent with that used in the Maier-Saupe theory.[26] Monte Carlo studies of this system showed a first-order transition from an orientationally ordered phase to a disordered one.[12–14] The effect of translational freedom on this model has also been studied where the above potential was used in conjunction with a Lennard-Jones interaction for the scalar component.[15] A weak first-order nematic-isotropic transition was found in Monte Carlo simulations. This model agreed well with the Maier-Saupe theory. Hard ellipses with full translational freedom have been studied in two dimensions and a transition to an orientationally ordered phase was found.[16] Other systems such as the hard ellipsoid of revolution[17,18] (HER) and prolate ellipsoids interacting with an orientation-dependent Lennard-Jones potential have been investigated.[19,20] Frenkel and co-workers have studied a HER fluid using Monte Carlo[17] and molecular-dynamics techniques.[18] They have observed the existence of four distinct phases: isotropic fluid, nematic fluid, ordered solid, and plastic solid. Kushick and Berne[19] have studied prolate ellipsoids in two dimensions using molecular-dynamics methods. The fluid was ordered using an imposed field; then the stability of the orientationally ordered phase without the field was investigated. For certain conditions, they found such phases to be stable. Other researchers employing the Berne-Pechukas-Kushick potential have observed a nematic phase in molecular-dynamics simulations.[21] Decoster, Costant, and Constant[20] have studied the influence of an off-center dipole in the prolate ellipsoid and have obtained indications of a partially bilayered smectic phase. Luckhurst, Simpson, and Zannoni[22] have simulated a lattice model for the smectic-*E* to -*B* transition. Stroobants, Lekkerkerker, and Frenkel[23] have used Monte Carlo techniques to investigate a system of hard spherocylinders whose long axes are constrained to lie in the same direction but whose centers of mass are free to translate. This is a model which starts out as a nematic fluid and they have observed a second-order like (continuous) transition to a stable smectic-*A* phase. Gunn and Dawson[24] have used the Gay-Berne overlap-model potential in molecular-dynamics calculations of lyotropic systems. Picken *et al.*[25] have used molecular dynamics to study the nematic phase of a realistic potential for 4-*n*-pentyl-4′-cyanobiphenyl.

In general, the more complicated the potential interactions used in the simulation of liquid-crystalline systems, the less of the phase diagram explored. This situation runs the gamut from lattice models which typically investigate the entire phase diagram of the model to the all-atom potential models which usually observe a single phase. One reason for this is that the numerical investigation of phase transitions is nontrivial because the approach to equilibrium becomes slower as a critical point is approached. Thus, a phase transition for a complicated molecule, such as a nematogen formed of a large organic molecule, is even more difficult. Second, the formation of a liquid-crystalline phase may require large-scale diffusion and rotation of complicated molecules making simulations computationally intensive. Such considerations have led researchers to the use of well-defined model systems that focus on the basic physics involved in the formation of a liquid-crystalline phase. Thus we see that the earliest models concentrated on the anisotropic interaction and sought to investigate only the orientational aspects of the phase transition. Similarly, simulation of the smectic-*E* to -*B* transition by Luckhurst, Simpson, and Zannoni[21] used as its model a system which was constrained by its very design to be only either smectic *E* or smectic *B*. Luckhurst, Simpson, and Zannoni[22] were focusing only on the destruction of the smectic-*E* orientational herringbone structure. Another example is the work of Stroobants, Lekkerkerker, and Frenkel[23] on hard spherocylinders with their long axes constrained to be aligned in the same direction. This work treated the nematic director as being already established and looked to find a transition to a smectic phase.

It is our intention to develop a simple simulation model, which can deal with molecular architectures such as those proposed in paper I. Thus, we want to consider a class of architectures composed of flexible and rigid segments. Furthermore, we want to devise a model in the same spirit as previous simulation work. We want to focus only on certain basic aspects of phase transitions involving such molecules and not attempt an out and out brute force simulation. We will consider two molecular architectures. The first will consist of a rigid segment with two flexible tails. This is the simplest architecture consisting of a combination of rigid and flexible segments (but not one that would form a ferroelectric phase). The second will be a molecule which consists of five segments: a long flexible, a short rigid, a short flexible, a long rigid, and a long flexible segment. The latter structure may form a ferroelectric phase according to the arguments in

I. As no dipoles will be considered in the model simulation, "ferroelectric" will be construed simply as "forming layers for which the layer plane is not a mirror plane." However, as will be discussed below, in this model most phases with polar layers will, in the infinite volume limit, have a definite layer ordering at any nonzero temperature.

We shall not concern ourselves with the isotropic nematic transition but will instead focus on the nematic-smectic transition. In this, we follow Stroobants, Lekkerkerker, and Frenkel[23] and consider a model wherein the molecules are already aligned, i.e., the nematic director is already established. The basic physics involved in the formation of the smectic layering for a rigid mesogen with two flexible tails has to do with the fact that the overlap of flexible segments with flexible segments on other molecules is entropically favored as opposed to the overlap of a flexible segment with a rigid segment. Thus, at high temperatures, there is a general disordering, but, as the temperature is lowered, this entropic distinction comes into play and layers are formed with flexible segments next to flexible segments and rigid segments next to rigid segments. We consider a model which is constrained to be either nematic or smectic. We have constructed a lattice model wherein the molecules can translate freely only in one direction and are otherwise constrained to a hexagonal lattice. We will refer to this system which has full translational freedom in one direction but a lattice in the other two as a quasilattice model. Thus, the molecules are already in an aligned (i.e., nematic) state. We have effected the entropic favoring of the flexible-flexible overlap by putting in an energetic penalty for a flexible-rigid overlap between neighboring molecules. Our model is similar to that of Stroobants, Lekkerkerker, and Frenkel[23] in that we constrain molecular orientations to be parallel to a chosen axis. It differs in that we consider more complicated molecular architectures through the inclusion of flexible segments and that we allow motion only along the nematic director.

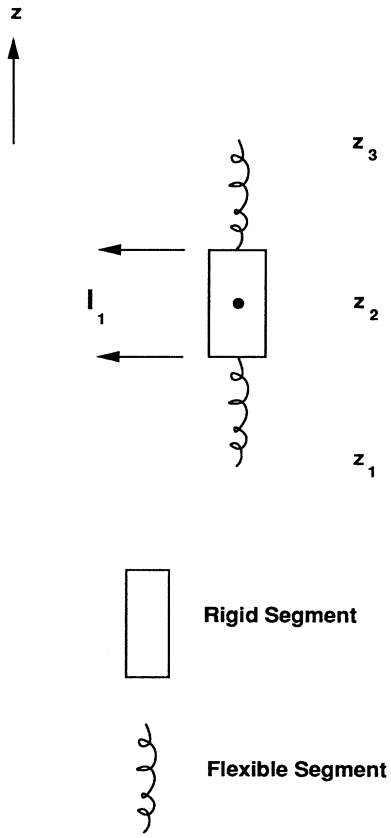

FIG. 2. Schematic of the molecular architecture for a simple, smectic former with one rigid section characterized by a length l_1 and and two flexible tails. We have termed this a FRF molecule. Such a molecule can be described by three independent sites which we have taken as the center of the rigid segment and the ends of the flexible tails. The molecules have translational freedom only along the z axis. The lines of translational freedom are arranged in a triangular lattice.

We initially consider the simple smectic-forming architecture of a rigid segment plus two flexible tails in order to (a) demonstrate that the model can display a nematic-smectic phase transition and (b) to develop a set of interaction parameters which will then be used for the more complicated molecular architecture which is proposed to have a ferroelectric phase. We are not interested in the precise details of the phase transitions such as, for example, the critical exponents. Rather, we wish to demonstrate a nematic-smectic phase transition, identify its location, and characterize the general nature of the transition. Then, using the *same* interaction parameters, consider the more complicated molecule and its possibly ferroelectric phase.

The outline of the rest of this paper is as follows. In Sec. II we describe in detail the model system and the method of simulation. In Sec. III we present simulation results for both molecules. In Sec. IV we conclude with a general discussion.

II. DESCRIPTION OF THE MODEL AND METHOD OF SIMULATION

The model consists of N molecules which have translational freedom along the z axis but are restricted to lie along lines parallel to that axis. The lines of translational freedom are arranged in a triangular lattice to reflect packing typical to smectics with in-plane order such as smectic B and a variety of rigid-rod systems. This, then is a quasilattice model in which the molecules are already aligned, i.e., the nematic director is already established. We have performed simulations on two classes of molecules. In the first class, each molecule is constructed out of a rigid, fixed-length segment with a flexible, variable-length segment attached to each end (Fig. 2). This is intended to represent a typical smectic-A-forming molecular architecture (e.g., a biphenyl with two attached alkane chains). We will refer to such an architecture as a flexible-rigid-flexible (FRF) type molecule. The second class of molecules has each molecule constructed of two rigid systems (not necessarily of equal length) connected by a flexible section, with flexible sections at each end as well (Fig. 3). Such a system is intended to represent molecular architectures which may be capable of forming

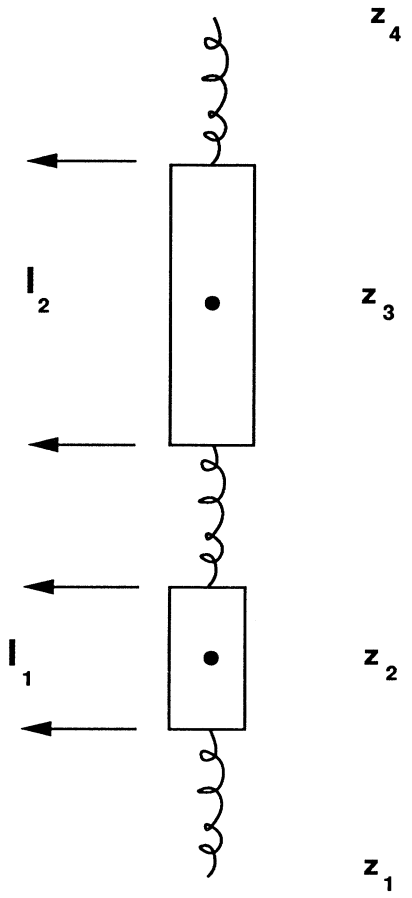

FIG. 3. Schematic of the molecular architecture suggested in I as being capable of forming a ferroelectric phase. We have termed this a FRFRF molecule. This molecule is characterized by two rigid sections of length l_1 and l_2 connected by a flexible segment with flexible tails on the ends of the molecules. This molecule is described by four independent sites given by the centers of the rigid sections and the ends of the molecule.

the ferroelectric phases discussed in the Introduction. We will designate these as FRFRF-type molecules. Both the molecules will be described by the z coordinates of their independent sites as shown in Figs. 2 and 3. These independent sites (three for FRF and four for FRFRF) can be taken to be the positions of the centers of the rigid segments and the (flexible) ends of the molecules. The length of the rigid sections are designated as l_i ($i=1$ for FRF and $i=1,2$ for FRFRF) and the separation between sites characterized by an equilibrium length a_i ($i=1,2$ for FRF and $i=1,2,3$ for FRFRF). Thus, the equilibrium length of a flexible segment is $a_i-l_1/2$ for the FRF molecule ($i=1,2$). For the FRFRF molecule, the flexible-segment lengths are $a_1-l_1/2$, $a_2-l_1/2-l_2/2$, and $a_3-l_2/2$. Since the molecules have translational freedom in the z direction, the model is further characterized by a length L in that direction. We can then describe a volume fraction defined by

$$\nu_f=M\left[\sum_{i=1}^{S} a_i\right]\Big/L \ , \tag{2.1}$$

where M is the number of molecules in the z direction, S is the number of sites and $\sum a_i$ is the noninteracting, zero temperature, equilibrium length of the molecule.

The separation between sites is governed by a harmonic potential

$$U_{\text{intra}}=\tfrac{1}{2}\gamma\sum_{\nu=1}^{S-1}(z_{i,\nu+1}-z_{i,\nu}-a_{i,\nu})^2 \ , \tag{2.2}$$

where $z_{i,\nu}$ is the νth site of molecule i and γ is the force constant. This reflects the entropic spring behavior of an alkane chain. The interaction between molecules on the same line of translational freedom ("z lines") is hard core, i.e., they are constrained not to overlap. Similarly, in addition to the harmonic potential, sites within a molecule are not allowed to pass through each other. Between molecules on nearest-neighbor z lines, the interaction is proportional to the amount of overlap between flexible and rigid segments

$$U_{\text{inter}}=\epsilon\Delta z_{ij} \ , \tag{2.3}$$

where Δz_{ij} is the total length over which the flexible segments of molecule i overlap the rigid ones of molecule j and vice versa (Fig. 4). The interaction parameter is ϵ. This interaction has been used to model smectic systems and reflects the additional entropy when flexible segments of molecules are next to other flexible segments rather than rigid ones.

The simulations were performed using the standard Monte Carlo algorithm of Metropolis *et al.*[27] A Monte Carlo step consisted of a trial movement of a molecule. There were two types of trial movements for the FRF molecule: molecular translations and molecular distortions. Because we are interested in the possibility of fer-

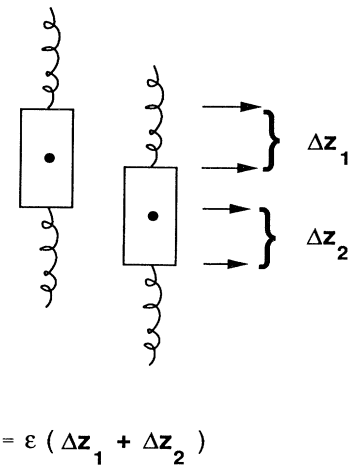

FIG. 4. Schematic of the energetic penalty used to favor the overlap of flexible with flexible and rigid with rigid segments on different nearest-neighbor molecules. This interaction is proportional to the amount of overlap between rigid and flexible segments.

roelectric phases, the FRFRF molecules had an additional trial movement, molecular inversions (to give them the possibility of pointing up or down). These trial moves are illustrated in Fig. 5. The molecular translations and distortions [Figs. 5(a) and 5(b)] are generated by

$$z_{\text{new}} = z_{\text{old}} \pm \xi\Delta \ , \tag{2.4}$$

where ξ is a uniformly distributed random number in the range (0,1) and the sign is chosen randomly. The maximum possible size for a trial move is Δ (Δ was adjusted to try and keep the accepted moves roughly between 40% and 70% of the attempted ones). The trial move z_{new} was either for the whole molecule (i.e., a translation preserving the current distances between the sites) or just one of the sites (i.e., a distortion of the molecular length). The molecular inversion consisted of inverting the molecule in such a fashion that there is no molecular distortion and that the end sites of the molecule are switched [Fig. 5(c)]. For the FRF molecule, molecular translations and distortions were selected each with probability equal to $\frac{1}{2}$. In the case of the FRFRF molecule, molecular translations, distortions, and inversions were chosen each with probability equal to $\frac{1}{3}$. It should be remarked that as inversions are a discrete motion it is impossible to adjust it so that it has a probability of success equal to $\frac{1}{2}$. At very low temperatures the inversion success rate was very small. At each trial move the energy change $\Delta U = U_{\text{new}} - U_{\text{old}}$ was calculated and the move was accepted or rejected depending on whether $e^{-\Delta U/kT}$ was greater or less than a random number uniformly distributed on (0,1). Selection of the molecule to undergo a trial move was done as follows: A randomly shuffled list of all the molecules was created. Molecules were taken sequentially from this list. A type of trial move was then selected and attempted. After reaching the end of the list, a new, shuffled list was created and the process repeated. We refer to this process as a cycle. Quantities to be averaged were calculated only at the end of each cycle. Periodic boundary conditions were employed in all directions.

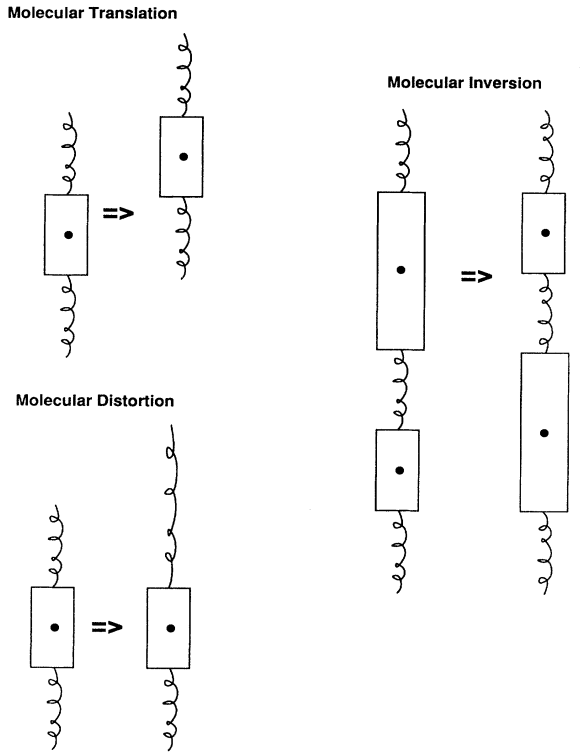

FIG. 5. Schematic of the different Monte Carlo moves used in the simulation. Molecular translation consists of translating the molecule as a whole along its direction of translational freedom (z axis). Molecular distortion consists of translating only one of the molecule's independent sites. Molecular inversion consists of inverting the molecule in such a fashion that there is no internal distortion and that the ends of the molecule are switched. Only translations and distortions were used with the FRF molecule, whereas translations, distortions, and inversions were used with the FRFRF molecule.

Table I contains the simulation parameters for the FRF and FRFRF molecule simulations. These length ratios were chosen to be within the usual range of molecules which are known to form smectic phases. In particular, if the shorter rigids are taken to be something like biphenyl then the flexibles are roughly seven carbon alkanes and the long rigids are roughly terphenyls. (Note that the FRF molecule is symmetric while the FRFRF molecule is asymmetric.) The simulations for the FRF molecules were started at a scaled temperature of $T^*=2.5$ ($T^*=kT/\epsilon$) in an ordered, layered configuration (i.e., smectic). The FRFRF molecules were also started in a smectic configuration at $T^*=2.5$ with their molecular orientations pointed in the same direction. In both cases, the final configuration from a run at a lower temperature was used as the starting configuration for a higher temperature run. Equilibration runs were typically 3000 cycles. Production runs (over which averages were calculated) were between 4000 and 20 000 cycles for the FRF molecule and between 8000 and 40 000 for the FRFRF molecule, with longer runs being used near phase transitions. These longer runs are required because the transitions are second order (or nearly second order) and there is appreciable critical slowing

TABLE I. Parameters for the FRF and FRFRF molecule simulations. NA means not applicable.

	FRF	FRFRF
Total no. of molecules	125	144
Number in z direction	5	4
Number in x-y direction	5×5	6×6
l_1	4.0	3.0
l_2	NA	6.0
a_1	5.5	5.5
a_2	5.5	7.5
a_3	NA	7.0
γ	2.0	2.0
ϵ	0.1	0.1
L	58.0	86.022
v_f	0.948	0.93

down. In some cases, several separate production runs at a given temperature would be averaged together (again, near the phase transition).

We have described the interactions within and between molecules as energetic in order to put the model into the context of a standard Monte Carlo simulation. However, we are describing largely entropic interactions. Therefore, the simulations are not really performed as a function of temperature but rather as a function of the entropic interaction parameter $\epsilon^* = \epsilon/kT$, where we have kept the ratio of the intramolecular interaction parameter to that of the intermolecular one, γ^*/ϵ^* constant. These entropic contributions depend on the actual temperature because the probability of a bend (gauche bond) in an alkane chain depends on temperature. Since it is perhaps more natural and convenient, we shall continue to refer to the quantity $(\epsilon^*)^{-1}$ as the "temperature," but it must be kept in mind that this is really the inverse of the entropic interaction parameter.

III. SIMULATION RESULTS

A. FRF molecule

Figure 6 shows a plot of the scaled average internal energy per particle $\langle U^* \rangle = \langle U \rangle / N\epsilon$ versus the scaled temperature T^* (angular brackets are used to denote an average). We first note that the energy increases in a continuous fashion. A change in curvature can be seen in the vicinity of $T^* = 15.0-17.5$, indicating a possible phase transition. We have also calculated the scaled heat capacity per particle given by

$$\langle C^* \rangle = \frac{C}{Nk} = \frac{\langle U^2 \rangle - \langle U \rangle^2}{kT^2} . \tag{3.1}$$

Fluctuation measurements are typically not very accurate

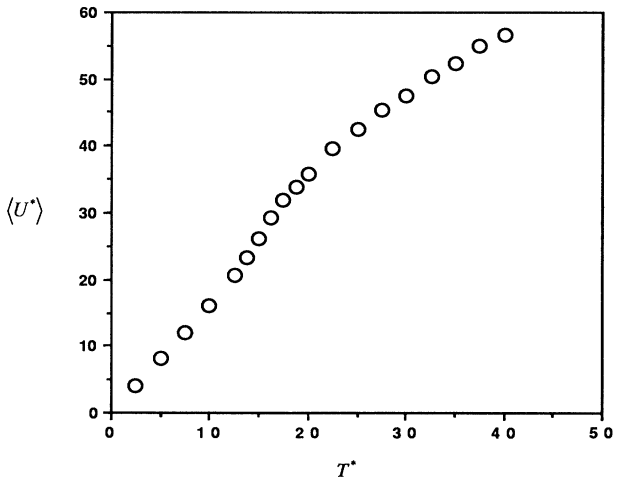

FIG. 6. Scaled energy vs scaled temperature for the FRF molecule. (Units used are dimensionless and are scaled with respect to the number of particles and energy parameter as described in the text.) Note the change of curvature at $T^* = 15.0-17.5$.

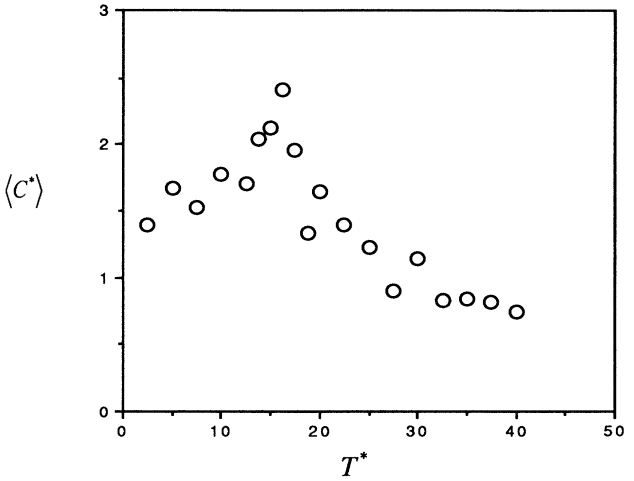

FIG. 7. Scaled heat capacity vs scaled temperature for the FRF molecule.

for simulations with a modest number of particles, but we can use this information to more precisely locate the phase transition by observing the maximum in $\langle C^* \rangle$. Figure 7 shows $\langle C^* \rangle$ versus T^*. This clearly shows a maximum which is located at $T^* = 16.25$. One can also calculate the specific heat by numerically spline fitting the $\langle U^* \rangle$ versus T^* curve to obtain $dU^*/T^* = C^*$. We have also done this calculation and it shows essentially the same peak as the fluctuation measurements. Thus far, the transition appears to be second order, i.e., continuous in U^* and discontinuous in C^*. However, it is difficult to draw unambiguous conclusions regarding the precise character of a phase transition because of finite-size effects. Since, as discussed in the Introduction, our goal is not such a characterization, we will simply note that our results are consistent with a second-order phase transition. This is expected on theoretical grounds as the nematic order parameter is strongly established and was also observed by Stroobants, Lekkerkerker, and Frenkel[23] in their work on hard spherocylinders.

We are, however, concerned with the transition as regards the nature of the liquid-crystalline phase. Figure 8 shows several "snapshots" of a plane of molecules on their lines of translation freedom for a series of temperatures ranging from below, near, and above the phase transition. These pictures were taken from the molecular configurations at the end of a production run for the given temperature. At the lowest temperature displayed ($T^* = 2.5$), the system shows a layered ordering typical to a smectic-A liquid-crystal phase. This ordering is strongly retained until we get to the transition temperature where the layers are no longer clearly defined. Note, however, that the system still shows evidence of layering. As we go past the transition temperature, we see that the system is no longer layered and has a molecular arrangement typical to nematics, i.e., no positional correlation between molecules on different lines of translational freedom. It is clear from these pictures that we can characterize the phase transition demonstrated by the behavior

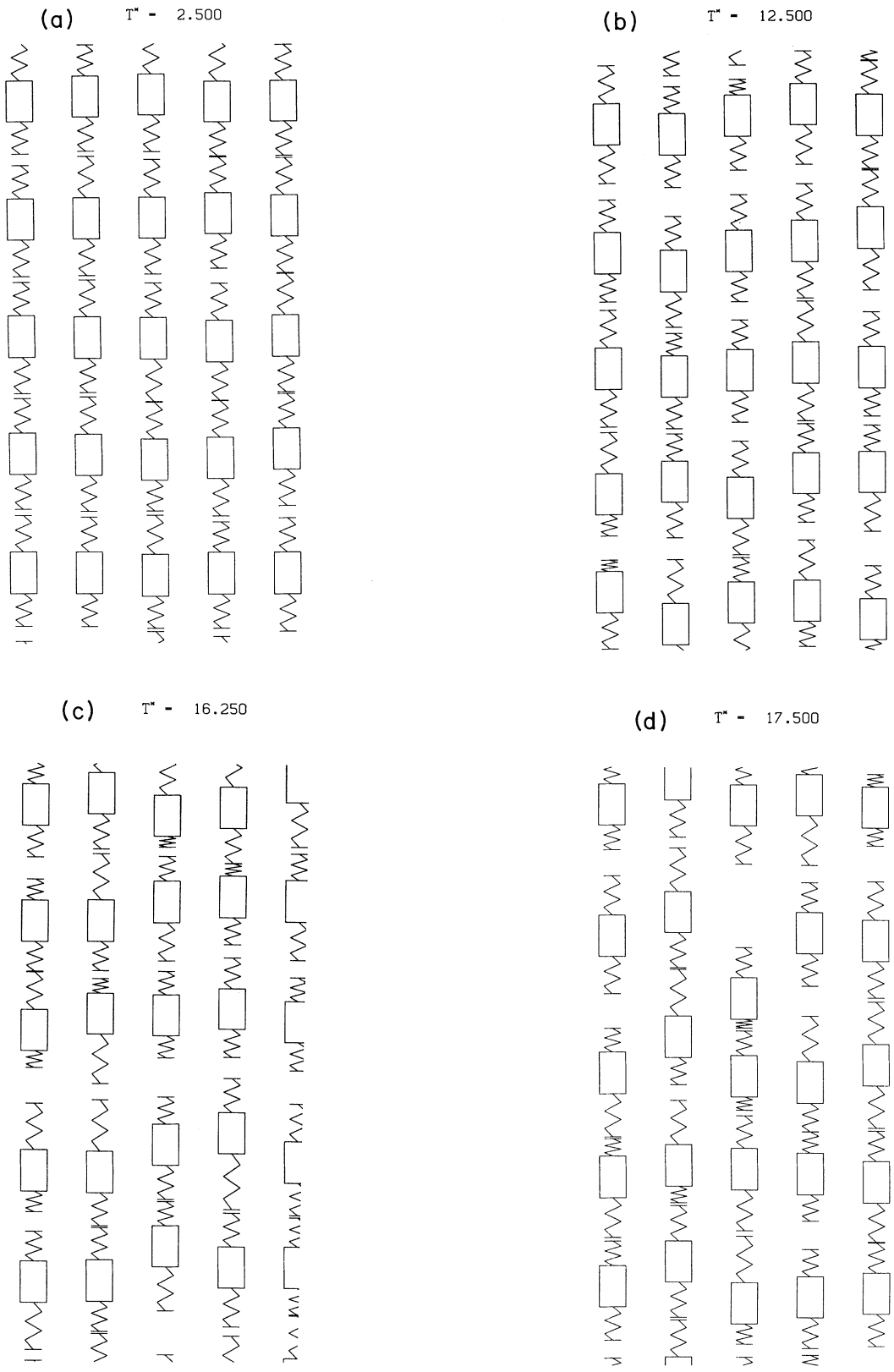

FIG. 8. "Snapshots" of a plane of FRF molecules on their lines of translational freedom for a series of temperatures below [(a) and (b)], near [(c)], and above [(d) and (e)] the transition temperature of 16.25. Note the destruction of the layer structure as the system is taken above the transition temperature.

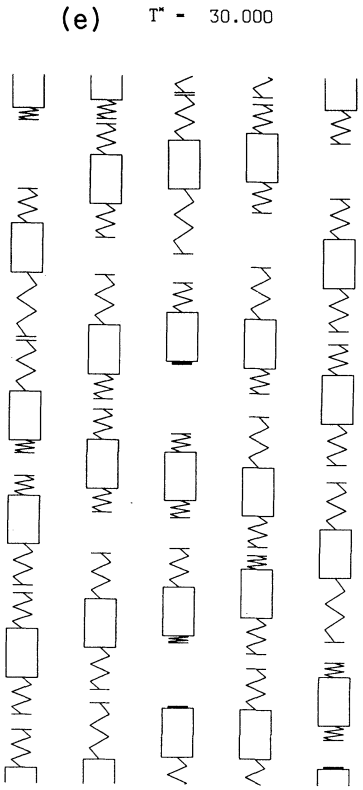

FIG. 8. (*Continued*).

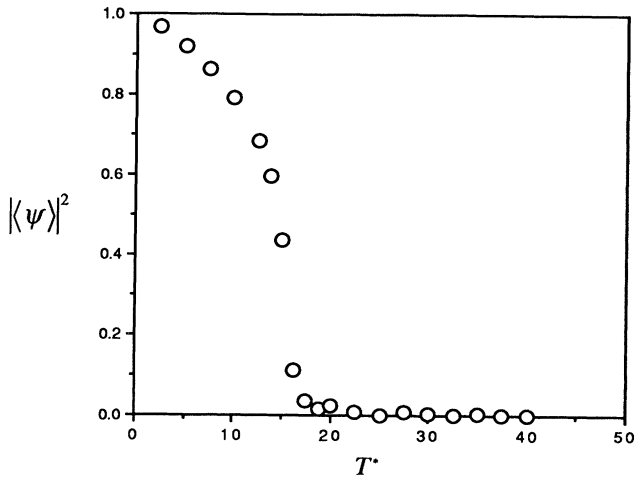

FIG. 9. Plot of the square of the average of the smectic order parameter for the FRF system as given by Eq. (3.4).

of $\langle U^* \rangle$ and $\langle C^* \rangle$ with temperature as a smectic-A to nematic transition.

A quantitative description of the transition from a layered smectic-A phase to a nematic one can be obtained through the use of an order parameter. To observe the formation of layers, we use the Fourier component of the position of the rigid portion of the FRF molecule, $z_{i,2}$ with respect to the layer spacing $k=2\pi M/L$, where M is the number of molecules on each line of translational freedom. Thus, we have for the order parameter

$$\psi=\frac{1}{N}\sum_{j=1}^{N} e^{iz_{j,2}k} , \tag{3.2}$$

and we calculate the average of the order parameter as we did for the energy. We will report on the square of the order parameter given by $|\langle\psi\rangle|^2=\langle\psi\rangle\langle\psi\rangle^*$, where the asterisk refers to the complex conjugate. There is one small complication about which we must be careful. For a small system such as ours, the system as a whole can translate. Such overall motion of the system will tend to "wash out" the value of the order parameter. To correct for this, we keep track of the center of mass of the system as defined by the rigid parts of the molecule and calculate the displacement of the center of mass

$$\Delta z_{\text{c.m.}}=z_{\text{c.m.}}-z^0_{\text{c.m.}} , \tag{3.3}$$

where $z_{\text{c.m.}}$ is the value of the center of mass at the beginning of the averaging for that run. (Note that in calculating the center of mass, it is important to account for the crossings of the periodic boundaries in the z direction.) Thus, the effect of overall motion of the system on the order parameter defined in Eq. (3.2) can be compensated for by redefining the order parameter as

$$\psi=e^{-i\Delta z_{\text{c.m.}}k}\left[\frac{1}{N}\sum_{j=1}^{N} e^{iz_{j,2}k}\right] . \tag{3.4}$$

Figure 9 plots the square of the average of this order parameter $|\langle\psi\rangle|^2$ versus T^*. At low temperatures, the order parameter is near 1. As the temperature increases, it gradually begins to drop and rapidly falls to zero in the vicinity of the transition temperature as defined by the heat capacity. The value of the order parameter does not go to zero at the transition temperature but shows a slight rounding off. Such behavior is typical of small systems and finite time simulations. Again, the character of the order parameter in the vicinity of the phase transition is consistent with that of a second-order transition. We can also locate the transition temperature more precisely by investigating the fluctuations in the order parameter, i.e., we consider

$$\langle\chi^2_\psi\rangle=\langle|\psi|^2\rangle-|\langle\psi\rangle|^2 . \tag{3.5}$$

This is essentially the susceptibility of the system to this periodic density wave. Figure 10 plots $\langle\chi^2_\psi\rangle$ versus T^*. Again, such fluctuation measurements are noisy, but a pronounced maximum at $T^*=16.25$ is observed, as was seen for the heat capacity.

B. FRFRF molecule

Figure 11 shows a plot of $\langle U^* \rangle$ versus $\langle T^* \rangle$ for the FRFRF molecule. As with the FRF molecule, the energy increases with temperature in a continuous fashion,

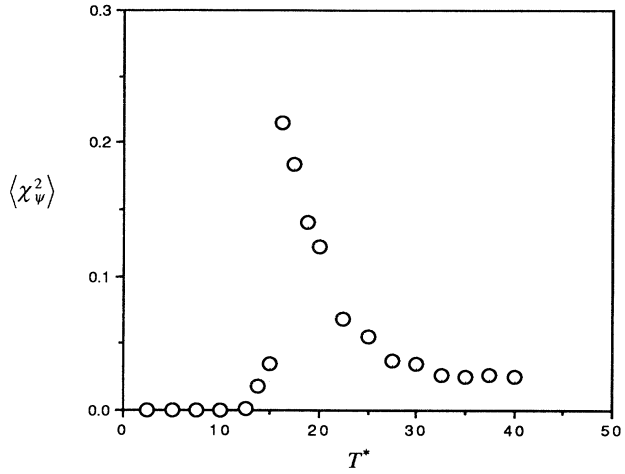

FIG. 10. Plot of the fluctuations in the smectic order parameter for the FRF system. Note that this peaks at the same temperature as the heat capacity.

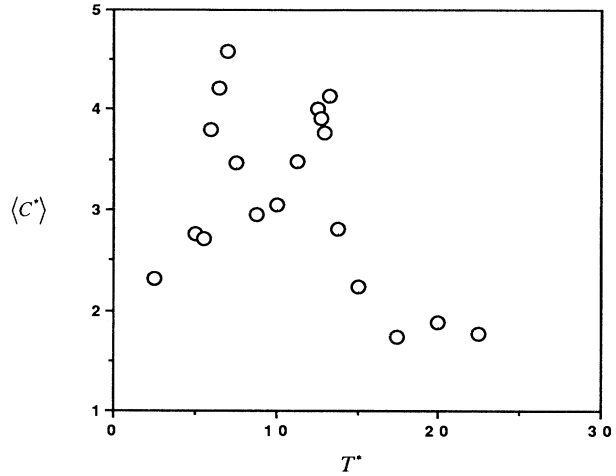

FIG. 12. Heat capacity vs temperature for the FRFRF system. Note that there are two peaks ($T^*=7.0$ and 13.25) indicating two phase transitions.

but now there appear to be two regions with a change in curvature. One is located in the range $T^*=6-8$ and the other around $T^*=12-15$. This indicates the possibility of two phase transitions. We turn to the heat capacity to more precisely locate these transitions, and this is shown in Fig. 12. The heat capacity versus temperature clearly shows two maxima, one at $T^*=7.0$ and the other at $T^*=13.25$. Both transitions are second order in nature.

We again look at snapshots of the system at various temperatures to help determine the character of the liquid-crystalline phases. Figure 13 shows pictures of the system at temperatures below, near, and above each of the transition temperatures indicated by the heat-capacity peaks. At the lowest temperatures, $T^*=2.5$, we see that the FRFRF molecules are in layers (smectic) and that their molecular orientations are all the same. That is, the molecules have their long rigid sections on "top." For convenience, we shall refer to such molecular orientations as "up" and the opposite as "down."

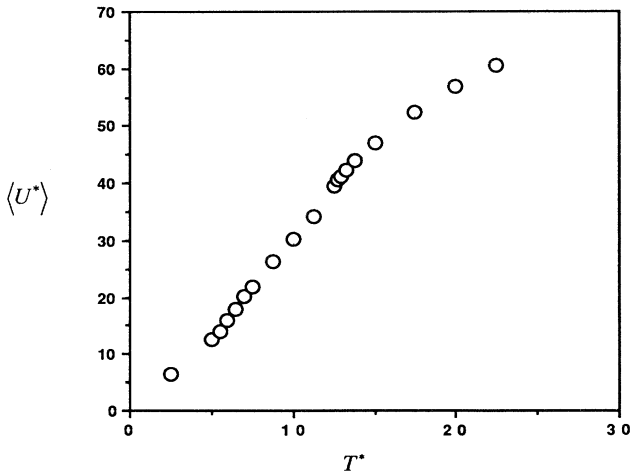

FIG. 11. Scaled energy vs scaled temperature for the FRFRF system. Note that there are two locations where the curvature changes; one at $T^*=6-8$ and the other at $T^*=12-15$.

Normally, this would be a ferroelectric phase except that the polarization would be zero, since there are no Coulombic interactions in this model. In addition, there is no energy difference between ferroelectric (all layers pointing in the same direction) and antiferroelectric (some layers pointing up, some down) phases. It is important, however, to remark that in this model most phases with polar layers will, in the infinite volume limit, have a definite layer ordering at any nonzero temperature. The fluctuations on one side of the layer will be different from those on the other side of the layer. These different fluctuations will then interact and except for particular values of various parameters, there will be a (slightly) lower free energy when the two similar layers are together (ferroelectric) or when the two different layers are together (antiferroelectric). As this free energy will be proportional to the area of the layers, it will, however small on a per molecule basis, result in a definite layer ordering in the thermodynamic limit. As these free-energy differences are small, our systems are small, and the rate at which our layers flip is observed to be small, this cannot be observed in these simulations. Such small free-energy differences can be studied by other methods.[28] In the model that has been studied in this paper, the fluctuations on either side are very similar and these free-energy differences are very, very small. In addition, as it is very difficult for a layer to flip over, it is not expected that a straightforward simulation will be able to distinguish between these two (or other) possible equilibrium situations but only between the polar and nonpolar phases. Any polar configuration is expected to persist, possibly with occasional flips to another polar configuration. It is this behavior which, in this simulation, will be characterized as a polar phase.

This distinction can be clearly seen by comparing the configurations near the polar-nonpolar transitions. At

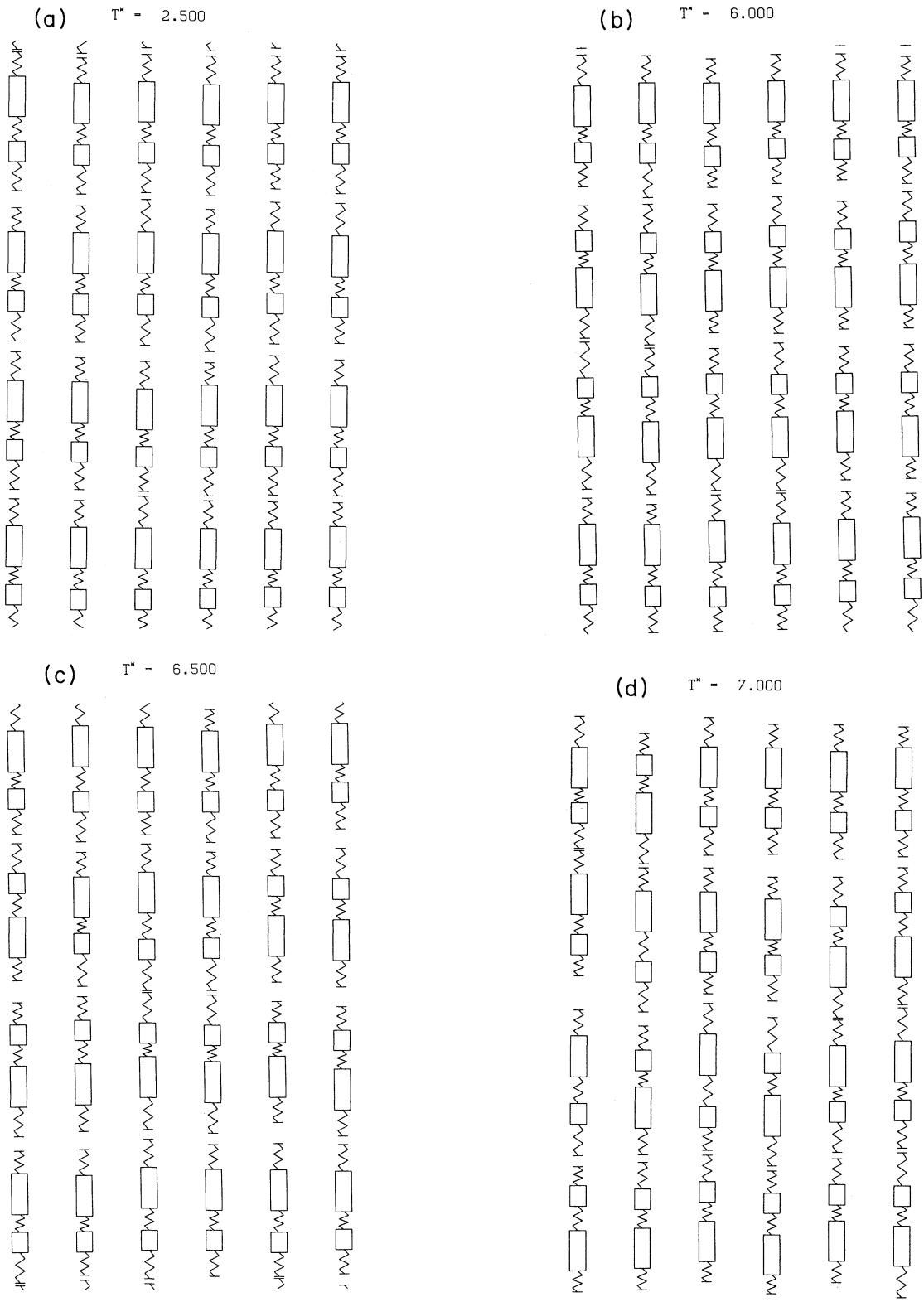

FIG. 13. "Snapshots" of a plane of FRFRF molecules on their lines of translational freedom for a series of temperatures below the first transition point, (a),(b),(c); at the first transition point, (d); between the transition points (e),(f),(g); at the second transition point, (h); and above the second transition point, (i). Note that for temperatures below the first transition point, (a) and (b), the layer order is retained and also the molecules point in the same direction within a layer (though the layers may alternate). Between the first and second transition points, (e)–(g), the layer structure is retained but there is "up-down" disorder within a layer. Finally, above the second transition point, (i), the layer structure is destroyed.

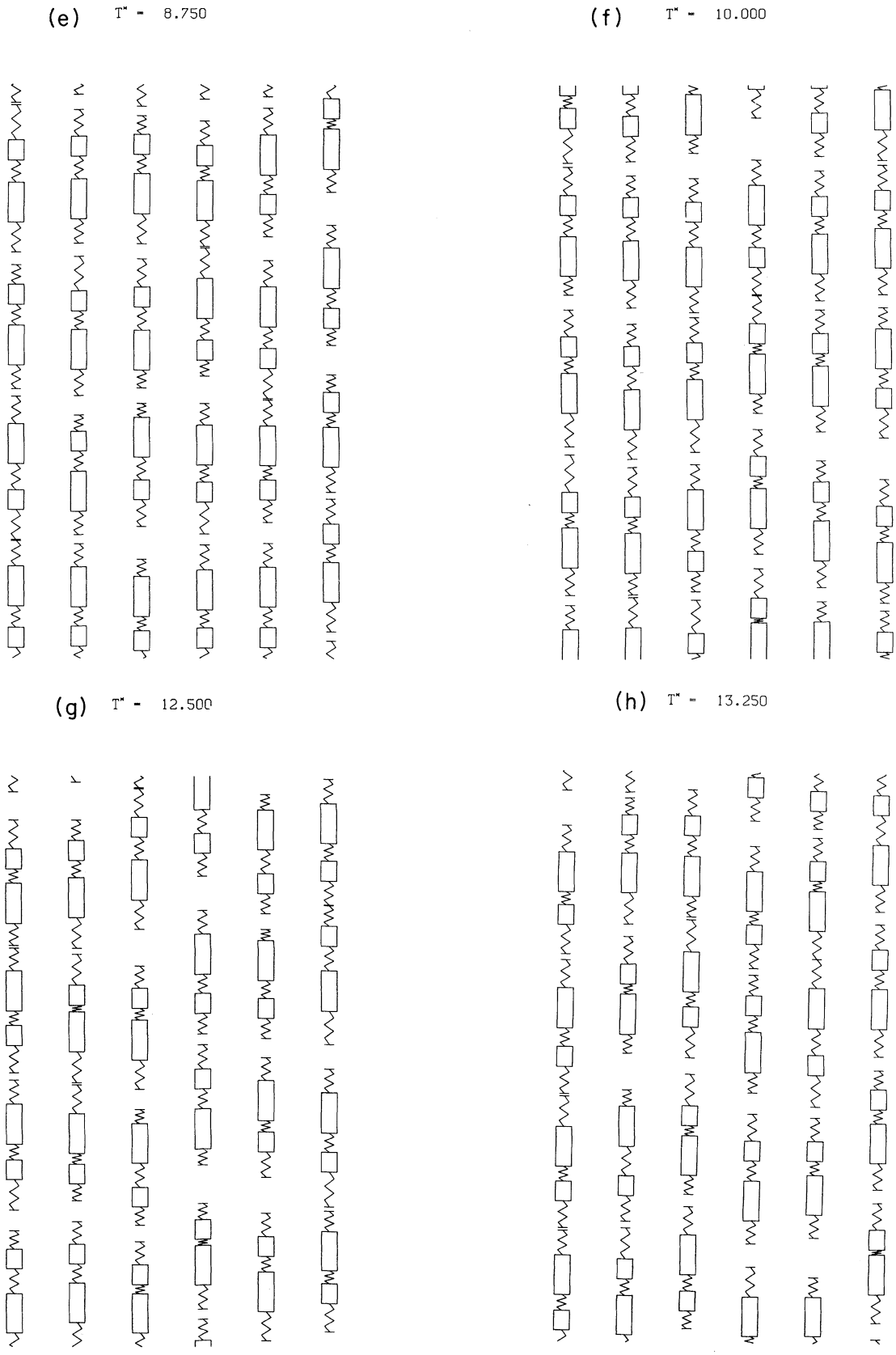

FIG. 13. (*Continued*)

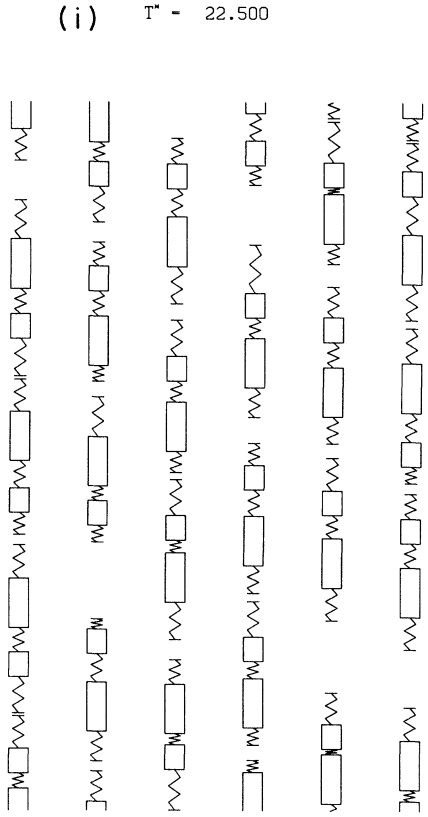

FIG. 13. (*Continued*).

$T^*=6$ we see that two of the layers (two and three from the bottom) have inverted and are now pointing down. The key point, though, is that *within* a layer, the molecules have the same orientation. That is, the layers retain their polar nature. At a slightly higher temperature, $T^*=6.5$, there are many occurrences of up and down molecules within the same layer (layer three from the bottom at $T^*=6.5$). This up-down disorder increases as we go through the phase transition at $T^*=7.0$ and the layers lose their polar nature. (At the transition point the inversion success ratio is still only $\sim 20\%$.) Continuing to move up in temperature, we see that the layer structure is beginning to disorder, and past the second transition temperature at $T^*=13.25$, we have destroyed the layer structure. This later transition is a smectic-A to nematic transition just as in the FRF molecule. The transition at $T^*=7.0$ is a polar transition because the molecules go from having like molecular orientations within layers to up-down disorder within layers (but still layered). We will refer to the low-temperature phase as smectic A_P for polar, the middle as smectic-A, and the high-temperature phase as nematic.

To be more quantitative, we must define order parameters. First we deal with the smectic order parameter. This is essentially the same as for the FRF molecule, the only difference being that we define two smectic order parameters: one based on the molecular center of mass

$$\psi_c = e^{-i\Delta z_{\text{c.m.}} k}\left[\frac{1}{N}\sum_{j=1}^{N} e^{ik_f z_{\text{c.m.}}^{\text{mol}}(j)}\right], \tag{3.6}$$

where $k_f=2\pi M/L$ and $z_{\text{c.m.}}^{\text{mol}}(j)$ is the molecular center of "mass" of molecule j as defined by the two rigid sections

$$z_{\text{c.m.}}^{\text{mol}}(j)=\tfrac{1}{2}(z_{j,2}+z_{j,3}) . \tag{3.7}$$

Care must be taken with respect to the periodic boundary conditions in evaluating Eq. (3.7). The correction for system center-of-mass movement is the same as before. The other smectic order parameter treats the rigid sections as individual elements and is given by

$$\psi_r = e^{-i\Delta z_{\text{c.m.}} k_r}\left[\frac{1}{2N}\sum_{j=1}^{N}(e^{iz_{j,2}k_r}+e^{iz_{j,3}k_r})\right], \tag{3.8}$$

where $k_r=4\pi M/L$.

Figure 14 shows $|\langle\psi_c\rangle|^2$ versus T^*. The order parameter is approximately unity at low temperatures and gradually decreases until in the vicinity of the phase transition at $T^*=13.25$, it falls to zero. The order parameter based on the molecular center of mass $|\langle\psi_c\rangle|^2$ displays characteristic second-order transition behavior. Figure 15 shows $|\langle\psi_r\rangle|^2$ versus T^*. Note that this order parameter is not unity at low temperature. This is because the rigid parts of the molecule cannot all lie on equally spaced layers. Thus the low-temperature (ordered) value of this order parameter will be different for different molecular architectures. The purpose of this order parameter was to look for the possible occurrences of layer structures formed of the type shown in Fig. 16. That is, rigid sections forming layers where the molecule was part of two layers and not just one. However, as seen from snapshots in Fig. 13 and the fact that $|\langle\psi_r\rangle|^2$ behaves in the same way as $|\langle\psi_c\rangle|^2$, dropping off to zero at the smectic phase transition temperature indicates that this alternative layering did not occur. We can also look at the fluctuations of Ψ_c and Ψ_r defined in the same manner as Eq. (3.5). These are shown in Figs. 17 and 18. The fluctuations of both the rigid and center-of-molecule order parameters

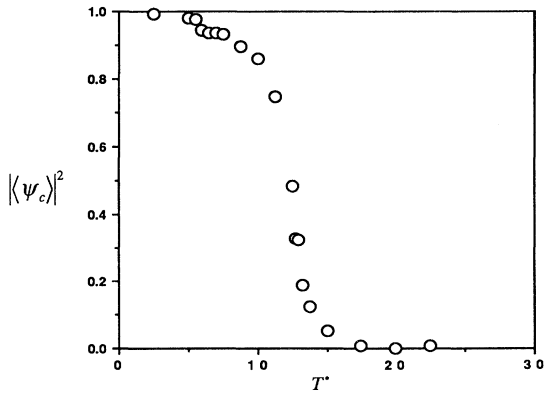

FIG. 14. Plot of the square of the average of the smectic order parameter based on the molecular centers of mass for the FRFRF system as given by Eq. (3.6).

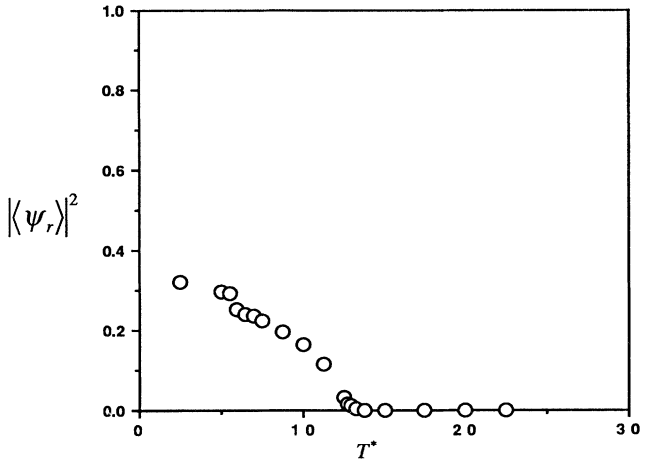

FIG. 15. Plot of the square of the average of the smectic order parameter based on the individual rigid segments for the FRFRF system as given by Eq. (3.8).

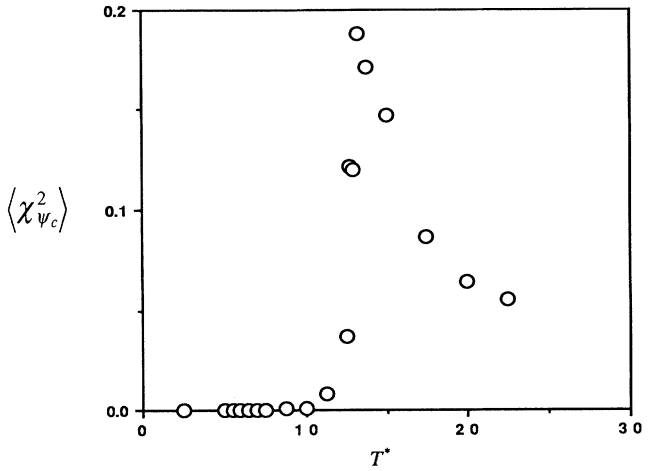

FIG. 17. Plot of the fluctuations in the smectic order parameter of Eq. (3.6) for the FRFRF system. Note that this peaks at (or near) the same temperature as the second transition point indicated by the heat capacity.

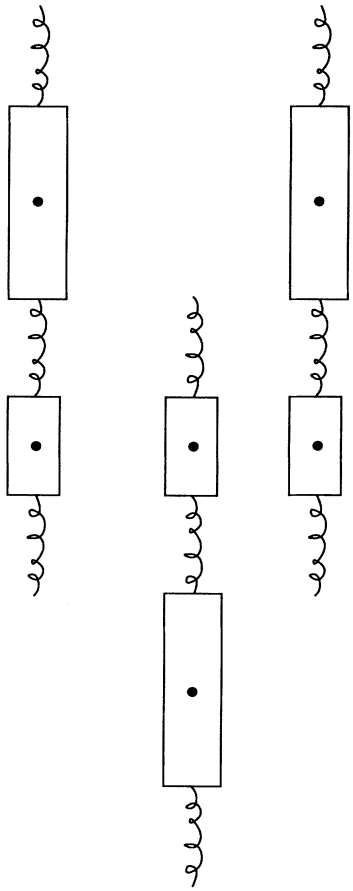

FIG. 16. A schematic of a possible layer structure. We did not see any evidence of such a layer configuration either in the snapshots of Fig. 13 or the order parameter of Fig. 15.

show strong peaks located at (or near) the transition temperature, $T^*=13.25$. There is a fair amount of scatter in the vicinity of the phase transition but it is clear that the transition occurs here.

Finally, we need a measure of the polar transition. For this we use

$$\psi_P=\frac{1}{N^2}\sum_{l=1}^{M-1}\left\{\left|\sum_{j=1}^{N}p_j e^{i2\pi(l/L)z^{\text{mol}}_{\text{c.m.}}(j)}\right|^2\right\}, \tag{3.9}$$

where $p_j=1$ if the molecular orientation is "up" and -1 if it is "down." This function has the properties that it is unity for perfect layered systems with either ferro- or antiferroelectric molecular orientations but goes to zero if there is up-down disorder within a layer. Figure 19

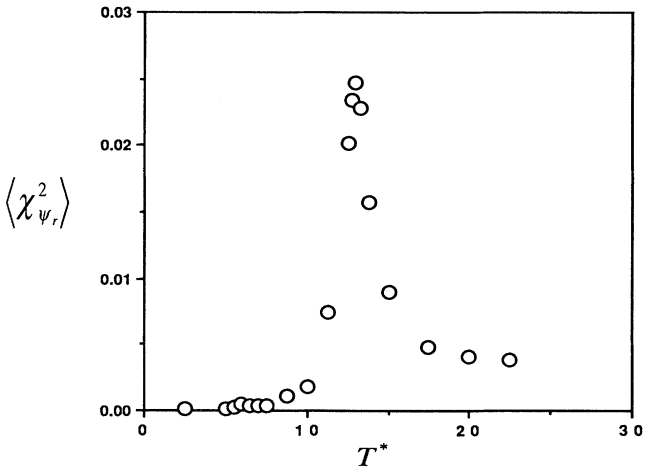

FIG. 18. Plot of the fluctuations in the smectic order parameter of Eq. (3.8) for the FRFRF system. Note that this peaks at (or near) the same temperature as the second transition point indicated by the heat capacity.

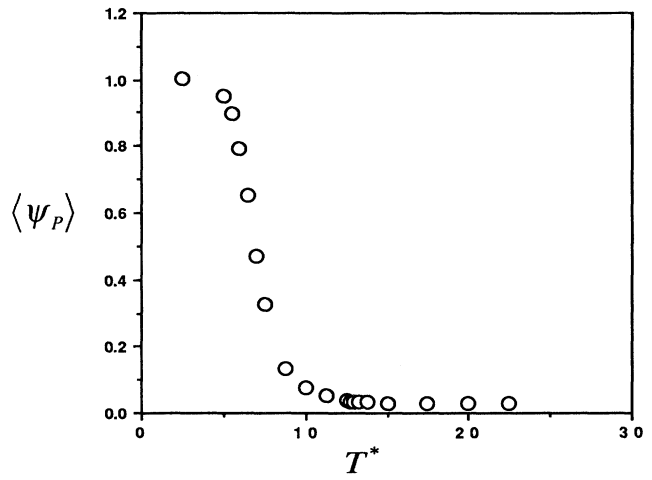

FIG. 19. Plot of the polar order parameter as given by Eq. (3.9) vs temperature for the FRFRF system. Note that this falls to zero in the vicinity of the first transition point indicated by the heat capacity.

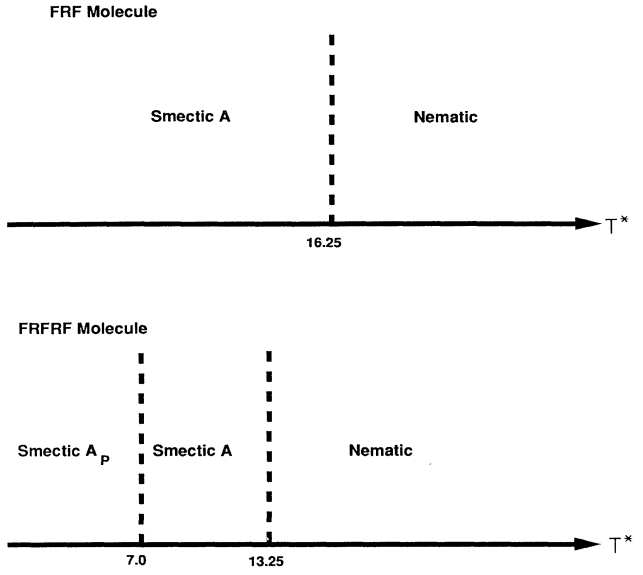

FIG. 20. Schematic phase diagram (roughly to scale) for the FRF and FRFRF systems.

shows $\langle \psi_P \rangle$ versus T^*. This polar order parameter goes to zero in the region of the transition marked by the peak in the heat capacity at $T^*=7.0$ and confirms the polar nature of this transition.

IV. DISCUSSION

We have summarized the results of the simulations for the FRF and FRFRF molecules in Fig. 20. We show a schematic phase diagram (drawn roughly to scale) for each of the molecular systems. The FRF molecule was comprised of a rigid section with two equal length flexible segments attached. For the parameters used, the FRF molecule has two phases: a low-temperature layered phase which can be characterized as smectic A and a high-temperature phase which is nematic. The transition temperature is at $T^*=16.25$ and the nature of the transition is second order as demonstrated by the fact that the energy varies continuously with temperature while the heat capacity shows a pronounced peak at the transition. This is consistent with experimental evidence for nematic-smectic phase transitions and also other simulations. The FRF molecule simulations were performed for two reasons: (1) To show that the quasilattice model could display such a smectic phase (and transition to the nematic phase) for a typical smectic-forming molecular architecture and (2) to develop the interaction parameters γ and ϵ (the intra- and intermolecular interaction parameters). For the FRFRF molecule, we used the same interaction parameters as for the FRF molecule. Only the molecular architecture (i.e., lengths and numbers of rigid and flexible segments) changed. Our goal was to determine the phase diagram for a molecular architecture (FRFRF) of the type suggested in paper I to form a ferroelectric phase given the interaction parameters, which, for a smectic-forming molecular architecture (FRF), resulted in the phase diagram of Fig. 20(a). The FRFRF molecule was found to have three phases. The low-temperature phase consists of layers of molecules which have like molecular orientations within a layer and the layers are arranged in either ferro- or antiferroelectric ordering. (Recall that there are no Coulombic interactions at this stage in the simulations—hence the ground state does not energetically favor one over the other.) We have termed this phase smectic A_p because of the polar nature of the molecular layers. The high-temperature phase is nematic with no layer ordering or ordering of molecular orientations. The middle phase has layer (smectic-A) ordering but also has orientational disorder within the layers. That is, the layers are nonpolar. These transitions occurred at $T^*=7.0$ for the smectic-A_p to smectic-A phase transition and at $T^*=13.25$ for the smectic-A to nematic transition. Both transitions displayed characteristics consistent with a second-order phase transition.

In comparing the two-phase diagrams, we note that the smectic-A–nematic transition temperature has been lowered for the FRFRF molecule from that of the FRF molecule by about 20%. This is reasonable as the FRFRF molecules have more ways in which to arrange themselves in a nonlayered fashion that does not cause as much flexible-rigid overlap as the FRF molecule. See Fig. 13 at temperatures $T^* \geq 13.25$, for example, where the FRFRF molecules have begun to disorder their layer structures. Compare this to the equivalent region in the FRF molecule (Fig. 8, $T^* \geq 16.25$). A second point to note is that although the smectic-nematic transition has been lowered, it has been lowered by a relatively small amount. Similarly, the polar phase persists to a fairly high temperature (approximately half the nematic-smectic transition temperature). These are very important points as we have found that a *reasonable* molecular architecture will generate a polar phase in a *reasonable* regime of the phase diagram. In other words, we did not

have to make the long rigid section huge compared to the short rigid section, nor did we find that the polar phase only existed at a very low (relative to the nematic-smectic transition) temperature. The arguments put forth by paper I for the existence of molecular architectures which would show ferroelectric phases are essentially symmetry arguments that can only argue for the *existence* of a phase and not whether that phase will exist in a reasonable (i.e., nontrivial) regime of the phase diagram. The simulations of the present work, we believe, add further credence to the symmetry arguments of paper I.

In conclusion, we have simulated a model liquid-crystal system which can display a smectic to nematic transition. Examination of a molecular architecture posited by Petschek and Wiefling to show a ferroelectric phase displays a polar smectic phase as well as the usual smectic and nematic phases. The degree to which these ideas and simulations reflect the behavior of real systems remains the subject of future work.

ACKNOWLEDGMENTS

This work was supported in part by the National Science Foundation through Grant No. DMR 89-01845 and by the Eastman Kodak Company Research Laboratories.

*Author to whom correspondence should be addressed.

[1]S. Chandrasekhar, *Liquid Crystals* (Cambridge University Press, New York, 1977).
[2]P. G. de Gennes, *The Physics of Liquid Crystals* (Clarendon, Oxford, 1974).
[3]S. Krause, Macromolecules **3**, 64 (1970).
[4]J. A. Manson, *Polymer Blends and Composites* (Plenum, New York, 1978).
[5]A. Blumstein, *Liquid Crystalline Order in Polymers* (Academic, New York, 1978).
[6]L. Liebert and L. Strzelecki, Bull. Soc. Chim. Fr. **2**, 603 (1973).
[7]R. B. Meyer, Mol. Cryst. Liq. Cryst. **40**, 33 (1977).
[8]R. G. Petschek and K. M. Wiefling, Phys. Rev. Lett. **59**, 343 (1987), hereafter referred to as I.
[9]P. Pallfy-Muhoray, M. A. Lee, and R. G. Petschek, Phys. Rev. Lett. **60**, 2303 (1988).
[10]Lin Lei, Mol. Cryst. Liq. Cryst. **146**, 41 (1987); L. M. Leung and Lin Lei, *ibid.* **146**, 71 (1987).
[11]M. P. Allen and M. R. Wilson, J. Comp.-Aided Mol. Design **3**, 335 (1989). This is an excellent review of computer simulations of liquid crystals with many fine references (and excellent illustrations).
[12]P. A. Lebwhol and G. Lasher, Phys. Rev. A **6**, 426 (1972); **7**, 2222 (1973).
[13]G. R. Luckhurst and P. Simpson, Mol. Phys. **47**, 251 (1982).
[14]U. Fabbri and C. Zannoni, Mol. Phys. **58**, 763 (1986).
[15]G. R. Luckhurst and S. Romano, Proc. R. Soc. London Ser. A **373**, 111 (1980).
[16]J. Vieillard-Baron, J. Chem. Phys. **56**, 4729 (1972).
[17]D. Frenkel and B. M. Mulder, Mol. Phys. **55**, 1171 (1985), and references therein.
[18]M. P. Allen and D. Frenkel, Phys. Rev. Lett. **58**, 1748 (1987), and references therein.
[19]J. Kushick and B. J. Berne, J. Chem. Phys. **64**, 1362 (1976).
[20]D. Decoster, E. Constant, and M. Constant, Mol. Cryst. Liq. Cryst. **97**, 263 (1983).
[21]A. L. Tsykalo and A. D. Bagmet, Mol. Cryst. Liq. Cryst. **46**, 111 (1978); D. J. Adams, G. R. Luckhurst, and R. W. Phippen, Mol. Phys. **61**, 1575 (1987).
[22]G. R. Luckhurst, P. Simpson, and C. Zannoni, Liq. Cryst. **2**, 313 (1987).
[23]A. Stroobants, H. N. W. Lekkerkerker, and D. Frenkel, Phys. Rev. Lett. **57**, 1452 (1986); Phys. Rev. A **36**, 2929 (1987).
[24]J. R. Gunn and K. A. Dawson, J. Chem. Phys. **91**, 6393 (1989).
[25]S. J. Picken, W. F. van Gunsteren, P. Th. vanDuijren, and W. H. deJeu, Liq. Cryst. **6**, 357 (1989).
[26]W. Maier and A. Saupe, Z. Naturforsch. **13**, 564 (1958).
[27]N. Metropolis, A. W. Rosenbluth, M. N. Rosenbluth, A. H. Teller, and E. Teller, J. Chem. Phys. **21**, 1087 (1953).
[28]J. Liu, R. G. Petschek, and D. R. Perchak (unpublished).